

# Electrical properties and sulfur tolerance of $\text{La}_{0.75}\text{Sr}_{0.25}\text{Cr}_{1-x}\text{Mn}_x\text{O}_3$ under anodic conditions

Shaowu Zha, Philip Tsang, Zhe Cheng, Meilin Liu\*

*School of Materials Science and Engineering, Georgia Institute of Technology, Atlanta, GA 30332-0245, USA*

Received 7 January 2005; received in revised form 17 March 2005; accepted 18 March 2005

Available online 18 April 2005

## Abstract

Complex metal oxides with composition of  $\text{La}_{0.75}\text{Sr}_{0.25}\text{Cr}_{1-x}\text{Mn}_x\text{O}_3$  ( $x = 0.4, 0.5, 0.6$ ) (LSCM) have been synthesized and examined as anode materials for solid oxide fuel cells (SOFCs). LSCM compositions show excellent tolerance to both reduction and oxidation but the crystal structure transforms from hexagonal in air to orthorhombic in  $\text{H}_2$ . The volume change associated with this phase transformation is only about 1%, thus having little effect on other properties. The total electrical conductivity increases with the content of Mn, whereas the resistance to sulfur poisoning increases with the content of Cr. Fuel cells using LSCM as the anode show very good performance when pure hydrogen is used as the fuel. However, they do not appear to be stable in fuels containing 10% of  $\text{H}_2\text{S}$ .

© 2005 Elsevier Inc. All rights reserved.

**Keywords:**  $\text{La}_{0.75}\text{Sr}_{0.25}\text{Cr}_{1-x}\text{Mn}_x\text{O}_3$ ; Electrical properties; Chemical stability; Solid oxide fuel cell; Sulfur-tolerant anode

## 1. Introduction

Doped lanthanum chromites (such as  $\text{La}_{1-x}\text{Sr}_x\text{CrO}_3$ ) have been widely investigated as interconnect materials for solid oxide fuel cells (SOFCs) because of their excellent stability and conductivity in both reducing and oxidizing atmospheres at elevated temperatures [1,2]. It was found that the introduction of other transitional metals into the B-site of  $\text{La}_{1-x}\text{Sr}_x\text{Cr}_{1-y}\text{M}_y\text{O}_3$  ( $M = \text{Mn}, \text{Fe}, \text{Co}, \text{Ni}$ ) could improve the catalytic properties for hydrocarbon reforming [3]. In addition, these double-doped perovskite phases are stable under redox (i.e., reduction–oxidation) cycling conditions with little volume change and are chemically and physically compatible with interconnect materials. Recently,  $\text{LaCrO}_3$ -based materials have been used as anodes in SOFCs fed with hydrocarbon fuels [4–7]. These materials have the potential to overcome the shortcoming of conventional Ni-based anode, which is confirmed to fail upon

repeated redox cycling and coking under hydrocarbon fuels. Furthermore, Ni-based anodes are readily susceptible to small amount of contaminants such as sulfur, a common contaminant in many hydrocarbon fuels. For example, approximately 10 ppm of sulfur-containing compounds is added to natural gas as an odorant. Thus, there is a need to develop sulfur-tolerant material for SOFCs to be operated on fuels with small amount of contaminants [8–12].

LSCM materials can be considered as solid solutions of  $\text{La}_x\text{Sr}_{1-x}\text{CrO}_3$  (LSC) and  $\text{La}_x\text{Sr}_{1-x}\text{MnO}_3$  (LSM). As a traditional interconnect material, LSC has high stability in an anodic environment. On the other hand, as a common cathode material, LSM has higher conductivity but is not stable in reducing atmosphere. In this communication, we report our results on the study of  $\text{La}_{0.75}\text{Sr}_{0.25}\text{Cr}_{1-x}\text{Mn}_x\text{O}_3$  (LSCM,  $x = 0.4, 0.5, 0.6$ ) as a potential anode material for SOFCs. In particular, their chemical and electrical properties are characterized to evaluate the feasibility of using them as anode in SOFCs. Moreover, the sulfur tolerance of the LSCM materials was examined

\*Corresponding author. Fax.: +1 404 894 9140.

E-mail address: [meilin.liu@mse.gatech.edu](mailto:meilin.liu@mse.gatech.edu) (M. Liu).

by introducing H<sub>2</sub>S (up to 10%) into hydrogen fuel stream.

## 2. Experimental

### 2.1. Powder preparation

Glycine nitrate combustion synthesis was used to prepare La<sub>0.75</sub>Sr<sub>0.25</sub>Cr<sub>0.6</sub>Mn<sub>0.4</sub>O<sub>3</sub> (LSCM64), La<sub>0.75</sub>Sr<sub>0.25</sub>Cr<sub>0.5</sub>Mn<sub>0.5</sub>O<sub>3</sub> (LSCM55), and La<sub>0.75</sub>Sr<sub>0.25</sub>Cr<sub>0.4</sub>Mn<sub>0.6</sub>O<sub>3</sub> (LSCM46) powders [13]. The molar ratio of glycine-to-metal ions was 2:1. After combustion, the foamy powders were calcined at 1200 °C in air for 2 h to remove residual carbon and promote complete crystallization of the perovskite phase, which was confirmed using X-ray diffraction (XRD, PW-1800 System,  $2\theta = 20\text{--}80^\circ$ ).

### 2.2. Conductivity measurements

The LSCM powders were dry pressed into bar samples (15 mm × 1 mm × 1 mm) and sintered at 1500 °C for 5 h to achieve relative density >95%. The conductivity of the bar samples was measured from 500 to 950 °C using a four-electrode dc technique in air, humidified (3% water vapor) H<sub>2</sub>, and 10% H<sub>2</sub>S (balanced by H<sub>2</sub>). For each gas, the sample was kept at 950 °C for 24 h before electrical measurements. Fig. 1 is a schematic of the four-electrode conductivity measurement setup. A Potentiostat/Galvanostat (273A, Princeton Applied Research) operating in galvanostatic mode was used to draw a constant dc current ( $I_i$ ) and a multimeter (Sinometer VC9807) was used to measure the voltage drop between the two inner

electrodes ( $\Delta V_i$ ). Five data points of ( $\Delta V_i, I_i$ ) were collected with different currents ( $I_i$ ) at each temperature. Linear fit (the least-squares method) was performed on the data to obtain the resistance.

### 2.3. Chemical stability examination

To test the stability of LSCM materials in H<sub>2</sub>S-containing atmosphere, pellets of LSCM were put in alumina boats placed in a tube furnace. The samples were then heated up to 950 °C and exposed to pure hydrogen or 10% H<sub>2</sub>S balanced by H<sub>2</sub> for 5 days. The post-treated pellets were then ground to powders for XRD analysis.

### 2.4. Fuel cell performance characterization

Yttria-stabilized zirconia ((ZrO<sub>2</sub>)<sub>0.92</sub>(Y<sub>2</sub>O<sub>3</sub>)<sub>0.08</sub>, YSZ) was cold-pressed at 250 MPa into cylindrical pellets using a uniaxial die-press, followed by sintering at 1550 °C for 5 h to obtain dense YSZ discs with 0.25 mm thickness. Ink consisting of LSCM55 and organic binder (V-006, Heraeus) was applied to one side of the YSZ electrolyte disc by screen-printing, followed by firing at 1300 °C in air for 2 h to form a porous anode. The cathode slurry, consisting of strontium-doped lanthanum manganate (LSM) and organic binder, was painted onto the opposite side of the YSZ disc and fired at 1250 °C in air for 2 h. Platinum mesh and wire (Heraeus) were attached to both electrodes as current collectors and the fuel cell was subsequently mounted to an alumina tube and sealed with ceramic adhesive (Flexbar Autostic). Electrochemical performance of the fuel cells

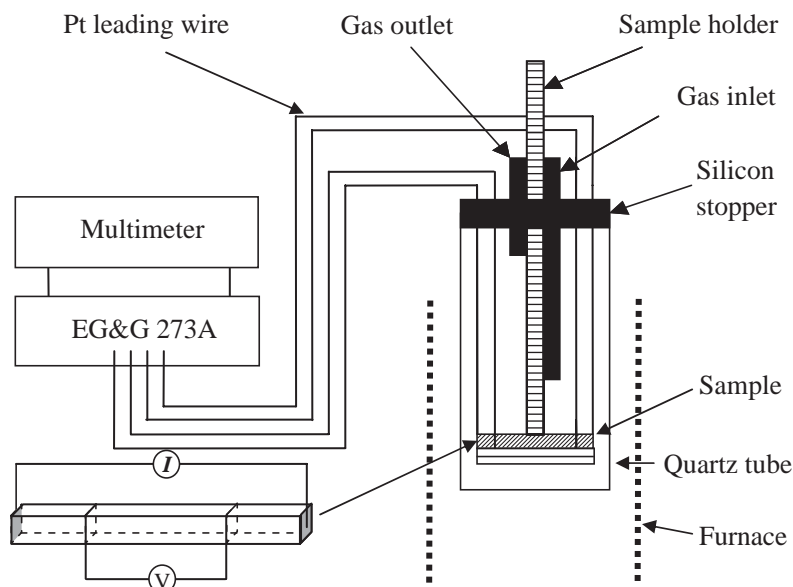


Fig. 1. Schematic illustration of the four-electrode dc conductivity measurement for anode materials.

were characterized using  $H_2$  and 10%  $H_2S$  (balanced by hydrogen) as fuels and stationary air as the oxidant at ambient pressure. The impedance was measured in a frequency range from 100 kHz to 0.01 Hz using an EG&G lock-in amplifier (Model 5210) and an EG&G Potentiostat/Galvanostat (Model 273A) interfaced with a computer. The fuel cell performance was acquired using CorrWare software.

### 3. Results and discussion

#### 3.1. Electrical conductivity

Shown in Fig. 2 are the typical conductivities of LSCM (bulk materials) measured using the four-electrode dc setup. The conductivities in air are one order of magnitude higher than those in hydrogen and sulfur-containing gas. The total conductivities of LSCM55 as measured at 900 °C in ambient air, wet  $H_2$ , and humidified  $H_2$  with 10%  $H_2S$  are 33.6, 1.7, and 1.6 S/cm, respectively. Similar to doped  $LaCrO_3$  interconnect materials, the conductivity of LSCM depends critically on the partial pressure of oxygen. In hydrogen, the oxygen loss reduces the carrier concentration and, thereby, decreases the conductivity of the LSCM materials [14]. However, under fuel cell operation conditions, large amounts of oxygen will be pumped from the cathode through electrolyte layer to the anode; thus, the anode conductivity may be significantly enhanced due to the increased oxygen partial pressure [15].

Shown in Fig. 3 are the conductivities of the LSCM samples as measured in both air and sulfur-containing

hydrogen gas between 500 and 950 °C. Once again, the conductivity is much higher in air than in 10%  $H_2S-H_2$  environment for all measured LSCM compositions. Consistent with the assumption that LSCM is a solid solution of LSC and LSM, the conductivity increases with the Mn content.

#### 3.2. Redox tolerance and phase stability

X-ray diffraction analysis of LSCMs, as shown in Fig. 4, indicates that all samples fired at 1200 °C in air are single-phase complex perovskites. The dense pellet samples show no change in morphology or color when heat-treated under redox conditions, i.e., exposed repeatedly to air and then hydrogen. However, the phase does convert between hexagonal ( $a = 5.4966 \text{ \AA}$ ,  $c = 13.3185 \text{ \AA}$ ) in air and orthorhombic ( $a = 5.5074 \text{ \AA}$ ,  $b = 5.4828 \text{ \AA}$ ,  $c = 7.7695 \text{ \AA}$ ) in  $H_2$ , accompanied by a small change in lattice parameter. This is why the conductivity changes significantly when the atmosphere is switched from air to  $H_2$ . The volume change is estimated to be about 1% for LSCM55 bulk material between oxidizing and reducing atmospheres at room temperature [7]. In contrast, the volume change is about 74% for oxidation of Ni to NiO and about 41% for reduction of NiO to Ni in a conventional Ni-YSZ anode. The LSCM55 anode shows excellent bonding with YSZ electrolyte under redox cyclings through our fuel cell preparation and testing.

Shown in Fig. 5 are the XRD patterns of LSCMs after being exposed to hydrogen sulfide up to 5 days. Some impurity phases, such as  $MnS$ ,  $La_2O_2S$  and  $\alpha$ - $MnOS$ , were visible after exposure, which resulted from

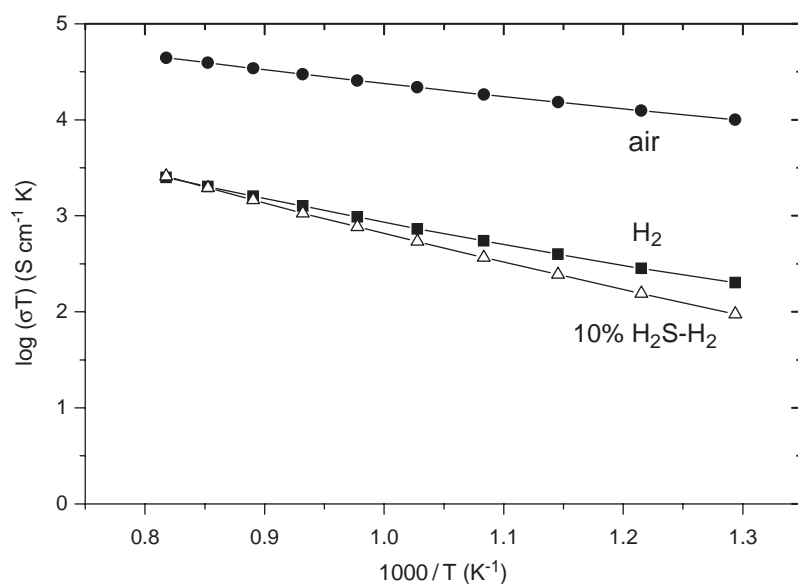


Fig. 2. Electrical conductivity of  $La_{0.75}Sr_{0.25}Cr_{0.5}Mn_{0.5}O_3$  (LSCM55) in (a) ambient air, (b) humidified  $H_2$ , and (c) humidified  $H_2$  with 10%  $H_2S$  at different temperatures.

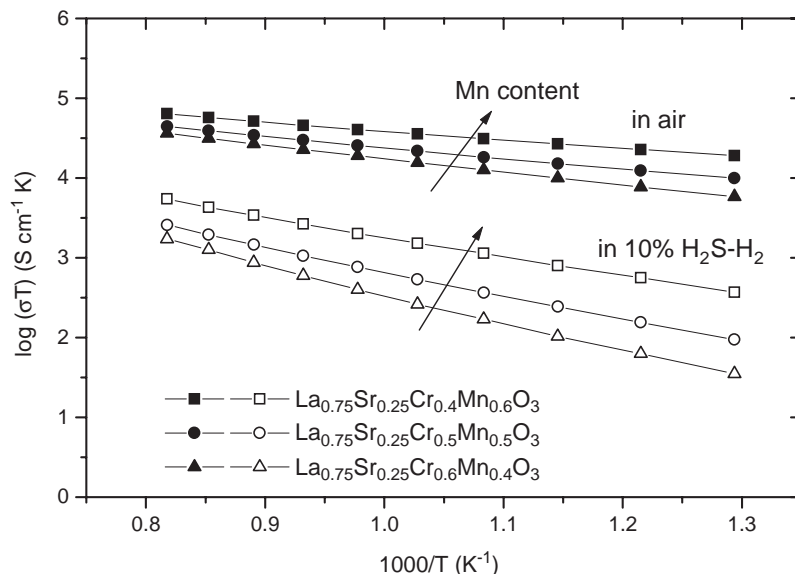


Fig. 3. Comparison of the total conductivities of LSCMs measured in ambient air and in humidified  $H_2$  with 10%  $H_2S$  (after the samples were exposed to the gas mixture at  $950^\circ C$  for 24 h).

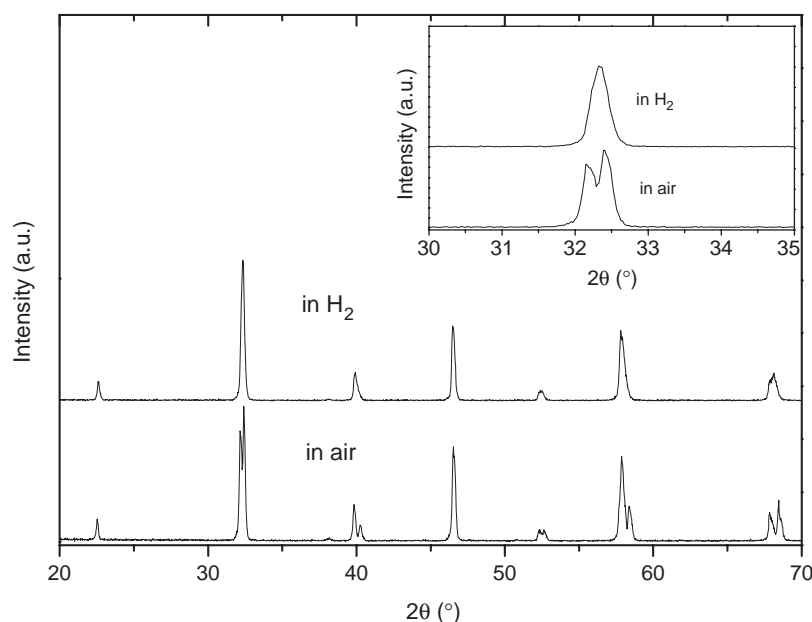


Fig. 4. XRD patterns of  $La_{0.75}Sr_{0.25}Cr_{0.5}Mn_{0.5}O_3$  (LSCM55) fired at  $1200^\circ C$  in air and hydrogen atmosphere. The inset shows the characteristic peaks that clearly demonstrate the phase conversion under redox environments.

the chemical reaction between LSCMs and  $H_2S$ . The amounts of the impurity phases decreased with the Cr content. The nonconductive phase,  $La_2O_2S$ , almost disappeared for the LSCM64 composition. As expected, the chemical stability of LSCM materials increased with the Cr content. However, the corresponding electrical conductivity decreased with the Cr content. In fact, the conductivity of LSCM64 is inadequate for electrode applications.

### 3.3. Fuel cell performance

The electrocatalytic properties, i.e., the activities towards electrochemical oxidation of fuel, of the LSCM perovskites were studied on YSZ electrolyte-supported cells consisting of a LSM cathode and LSCM55 anode (the thickness of the YSZ electrolyte was about 0.25 mm). Typical current–voltage characteristics and the corresponding power densities are shown in Fig. 6.

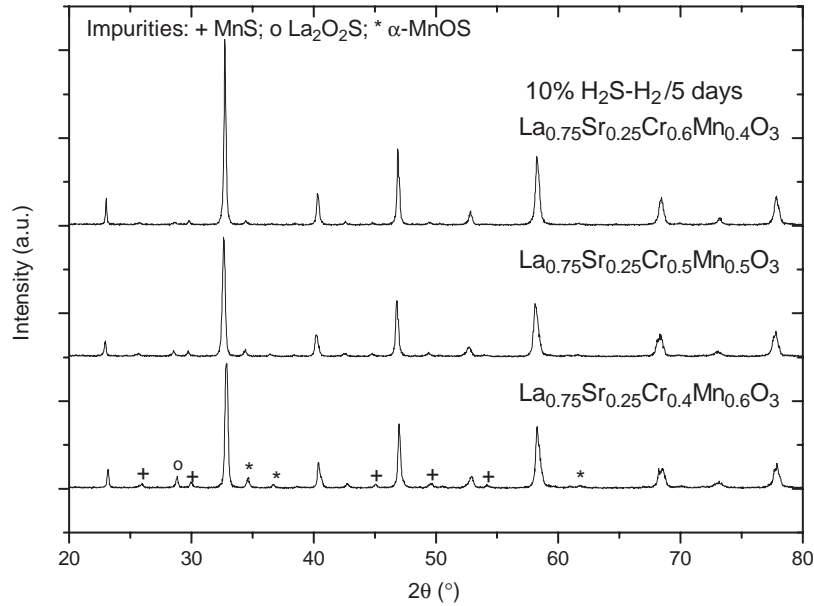


Fig. 5. XRD patterns of LSCMs after being exposed to humidified  $H_2$  containing 10%  $H_2S$  at  $950^\circ C$  for 5 days.

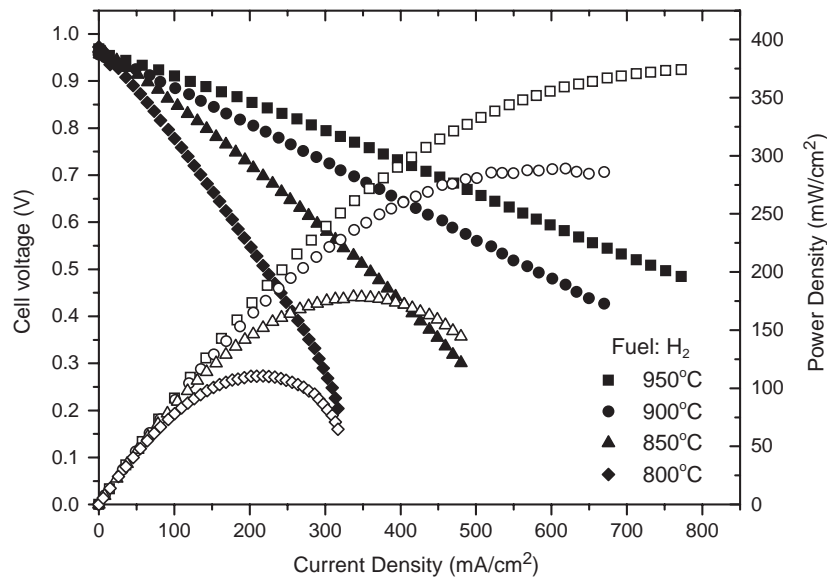


Fig. 6. Fuel cell performance with  $La_{0.75}Sr_{0.25}Cr_{0.5}Mn_{0.5}O_3$  (LSCM55) as anode at different temperatures. The fuel gas was humidified hydrogen (3%  $H_2O$  vapor) at a flow rate of 20 ml/min and the cathode was exposed to stationary air.

The fuel cell demonstrates excellent performance when running on moisturized hydrogen fuel. A steady-state performance was attained after the fuel cell was running on  $H_2$  for more than 24 h. Peak power densities of 280 and  $375 \text{ mW/cm}^2$  were obtained at 900 and  $950^\circ C$ , respectively.

Impedance spectra were acquired using both two-electrode and three-electrode configurations under open circuit conditions in order to separate the resistance of each cell component: the electrolyte, anode, and

cathode. Shown in Fig. 7 are some typical impedance spectra collected at  $950^\circ C$  under open circuit conditions. The total interfacial polarization resistance can be separated into two parts: the anode–electrolyte interfacial resistance and the cathode–electrolyte interfacial resistance. The anodic polarization resistance was about  $0.17 \Omega \text{ cm}^2$  at  $950^\circ C$ , while the cathodic polarization resistance was about  $0.28 \Omega \text{ cm}^2$ . The anodic and cathodic polarization resistances may be further reduced by optimizing both the microstructure and composition

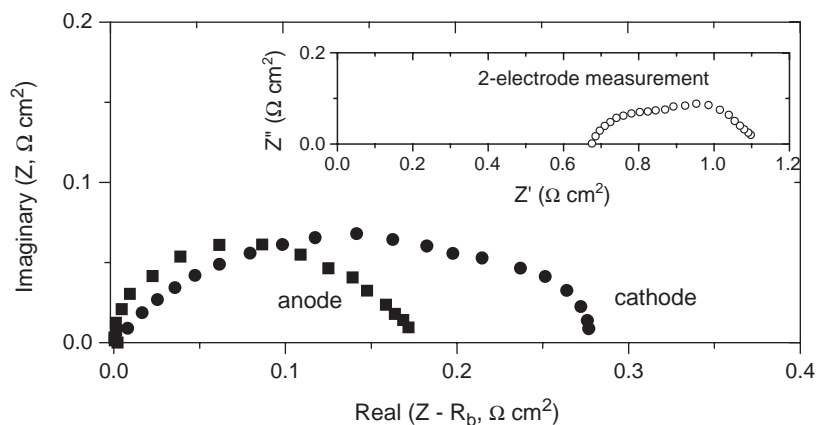


Fig. 7. Impedance spectra of electrolyte–anode (LSCM55) and electrolyte–cathode (LSM) interfaces under open circuit conditions at 950 °C. The inset shows the impedance spectra of the whole cell measured using a two-electrode configuration.

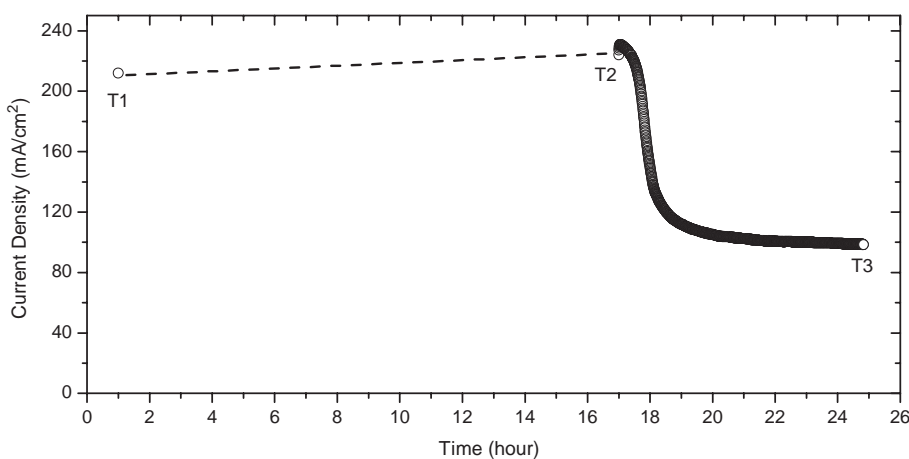


Fig. 8. Current change with time for an SOFC with LSCM55 anode operated on humidified H<sub>2</sub> with 10% H<sub>2</sub>S at 950 °C. The cell was under open circuit condition from T1 to T2, whereas the cell voltage was kept at 0.7 V from T2 to T3.

of the electrodes. It should be noted that the ohmic drop of the electrolyte (of 0.25 mm thick) is as high as 0.67 Ω cm<sup>2</sup> at 950 °C, which is about 60% of the total resistance of the cell. Thus, higher power densities are expected when a thinner electrolyte is used.

The LSCM55 anode was also tested in fuels containing high concentrations of H<sub>2</sub>S. As shown in Fig. 8, 210 mA/cm<sup>2</sup> was drawn from the cell at 0.7 V after flowing 10% H<sub>2</sub>S–H<sub>2</sub> fuel to the anode chamber at 950 °C for 1 h (labeled as point T1 in the figure). The cell was then kept under open circuit condition for another 16 h, after which the current density increased to 220 mA/cm<sup>2</sup> at 0.7 V (point T2). From T2 to T3 (8 h total), the fuel cell was operated at a constant cell voltage of 0.7 V. After a small initial increase, the cell performance dropped quickly to about half of the original performance in a 2-h period. This quick drop may be attributed to the intensified poisoning effect of sulfur on the LSCM55 anode under the electrochemical

oxidation conditions. Under open circuit condition, only chemical reactions will take place between anode materials and hydrogen sulfide as discussed earlier. These reaction rates are relatively slow even at very high H<sub>2</sub>S concentration and elevated temperature (950 °C). It is also interesting to note that the reaction products (such as MnS and MnOS) are conductive, which can reduce the electrode sheet resistance and, as a result, improve the current collection. This may explain the phenomenon that the performance has a small increase after the cell was fed with sulfur-containing fuel for 17 h (from T1 to T2). When the cell operated under the potentiostatic condition, however, the electrochemical oxidation dominates the reactions of H<sub>2</sub>S and H<sub>2</sub> with the oxygen pumped to the anode via electrolyte. The intermediate species and final products may accelerate the poisoning effect on anode materials, especially near the triple-phase boundaries (TPB), and degrade the cell performance rapidly to a much lower level (see T3 in

Fig. 8). A possible remedy is to protect the LSCM anode with a thin layer of sulfur-tolerant materials such as Sr-doped lanthanum titanates and vanadates [11,16].

#### 4. Conclusions

We have synthesized and characterized  $\text{La}_{0.75}\text{Sr}_{0.25}\text{Cr}_{1-x}\text{Mn}_x\text{O}_3$  ( $x = 0.4, 0.5, 0.6$ ) as a potential anode material for solid oxide fuel cells under both pure hydrogen and  $\text{H}_2\text{S}$ -containing atmospheres. The crystal structure changes from hexagonal in air to orthorhombic in  $\text{H}_2$  for all LSCM compositions. This transformation is accompanied by only a 1% volume change, indicating very good structural stability under redox conditions. The total conductivity of LSCMs increases with the Mn content within the temperature range studied (500–950 °C), and is about one order of magnitude higher in air than in a reducing atmosphere. Some impurity phases, such as MnS,  $\text{La}_2\text{O}_2\text{S}$  and  $\alpha$ -MnOS, are formed after LSCM was exposed to 10%  $\text{H}_2\text{S}$ - $\text{H}_2$  for 5 days. The amounts of the impurity phases decreased with Cr content. The fuel cell demonstrates very high performance with  $\text{H}_2$  fuel; the anodic polarization resistance was only  $0.17 \Omega \text{cm}^2$  at 950 °C, yielding a peak power density of  $375 \text{mW/cm}^2$ .

#### Acknowledgments

This work was supported by Department of Energy (Grant DE-FC26-04NT42219). One of the authors (P.

Tsang) would like to acknowledge the support of NSF SURF program (Summer, 2004).

#### References

- [1] N.Q. Minh, *J. Am. Ceram. Soc.* 76 (1993) 563–588.
- [2] H.U. Anderson, F. Tietz, in: S.C. Singhal, K. Kendall (Eds.), *High Temperature Solid Oxide Fuel Cells: Fundamentals, Design, and Applications*, Elsevier, Oxford, New York, 2003, p. 174.
- [3] J. Sfeir, P.A. Buffat, P. Mückli, N. Xanthopoulos, R. Vasquez, H.J. Mathieu, J. Van herle, K.R. Thampi, *J. Catal.* 202 (2001) 229–244.
- [4] P. Vernoux, J. Guindet, M. Kleitz, *J. Electrochem. Soc.* 145 (1998) 3487–3492.
- [5] S. Primdahl, J.R. Hansen, L. Grahl-Madsen, P.H. Larsen, *J. Electrochem. Soc.* 148 (2001) A74–A81.
- [6] J. Liu, B.D. Madsen, Z. Ji, S.A. Barnett, *Electrochem. Solid-State Lett.* 5 (2002) A122–A124.
- [7] S. Tao, J.T.S. Irvine, *J. Electrochem. Soc.* 151 (2004) A252–A259.
- [8] Y. Matsuzaki, I. Yasuda, *Solid State Ionics* 132 (2000) 261–269.
- [9] O.A. Marina, N.L. Canfield, J.W. Stevenson, *Solid State Ionics* 149 (2002) 21–28.
- [10] M. Liu, G. Wei, J. Luo, A.R. Sanger, K.T. Chuang, *J. Electrochem. Soc.* 150 (2003) A1025–A1029.
- [11] R. Mukundan, E.L. Brosha, F.H. Garzon, *Electrochem. Solid-State Lett.* 7 (2004) A5–A7.
- [12] L. Aguilar, S. Zha, S. Li, M. Liu, J. Winnick, *Electrochem. Solid-State Lett.* 7 (2004) A324–A326.
- [13] L.A. Chick, L.R. Pederson, G.D. Maupin, J.L. Bates, L.E. Thomas, G.J. Exarhos, *Mater. Lett.* 10 (1990) 6–12.
- [14] N.Q. Minh, T. Takahashi, *Science and Technology of Ceramic Fuel Cells*, Elsevier Science B.V., 1994, p. 175.
- [15] S. Zha, C. Xia, G. Meng, *J. Appl. Electrochem.* 31 (2001) 93–98.
- [16] L. Aguilar, S. Zha, Z. Cheng, J. Winnick, M. Liu, *J. Power Sources* 135 (2004) 17–24.